AMERICAN SOCIETY FOR MICROBIOLOGY | mSphere®

RESEARCH ARTICLE

Loss of β-Ketoacyl Acyl Carrier Protein Synthase III Activity Restores Multidrug-Resistant *Escherichia coli* Sensitivity to Previously Ineffective Antibiotics

Yaoqin Hong,[a] Jilong Qin,[a] Anthony D. Verderosa,[a]* Sophia Hawas,[a] Bing Zhang,[b] Mark A. T. Blaskovich,[b] John E. Cronan, Jr.,[c,d] Makrina Totsika[a]

[a]Centre of Immunology and Infection Control, School of Biomedical Sciences, Faculty of Health, Queensland University of Technology, Brisbane, Queensland, Australia
[b]Centre for Superbug Solutions, Institute for Molecular Bioscience, University of Queensland, Brisbane, Queensland, Australia
[c]Department of Microbiology, School of Molecular and Cellular Biology, University of Illinois at Urbana-Champaign, Urbana, Illinois, USA
[d]Department of Biochemistry, School of Molecular and Cellular Biology, University of Illinois at Urbana-Champaign, Urbana, Illinois, USA

ABSTRACT Antibiotic resistance is one of the most prominent threats to modern medicine. In the latest World Health Organization list of bacterial pathogens that urgently require new antibiotics, 9 out of 12 are Gram-negative, with four being of "critical priority." One crucial barrier restricting antibiotic efficacy against Gram-negative bacteria is their unique cell envelope. While fatty acids are a shared constituent of all structural membrane lipids, their biosynthesis pathway in bacteria is distinct from eukaryotes, making it an attractive target for new antibiotic development that remains less explored. Here, we interrogated the redundant components of the bacterial type II fatty acid synthesis (FAS II) pathway, showing that disrupting FAS II homeostasis in *Escherichia coli* through deletion of the *fabH* gene damages the cell envelope of antibiotic-susceptible and antibiotic-resistant clinical isolates. The *fabH* gene encodes the β-ketoacyl acyl carrier protein synthase III (KAS III), which catalyzes the initial condensation reactions during fatty acid biosynthesis. We show that *fabH* null mutation potentiated the killing of multidrug-resistant *E. coli* by a broad panel of previously ineffective antibiotics, despite the presence of relevant antibiotic resistance determinants, for example, carbapenemase *kpc2*. Enhanced antibiotic sensitivity was additionally demonstrated in the context of eradicating established biofilms and treating established human cell infection *in vitro*. Our findings showcase the potential of FabH as a promising target that could be further explored in the development of therapies that may repurpose currently ineffective antibiotics or rescue failing last-resort antibiotics against Gram-negative pathogens.

IMPORTANCE Gram-negative pathogens are a major concern for global public health due to increasing rates of antibiotic resistance and the lack of new drugs. A major contributing factor toward antibiotic resistance in Gram-negative bacteria is their formidable outer membrane, which acts as a permeability barrier preventing many biologically active antimicrobials from reaching the intracellular targets and thus limiting their efficacy. Fatty acids are the fundamental building blocks of structural membrane lipids, and their synthesis constitutes an attractive antimicrobial target, as it follows distinct pathways in prokaryotes and eukaryotes. Here, we identified a component of fatty acid synthesis, FabH, as a gate-keeper of outer membrane barrier function. Without FabH, Gram-negative bacteria become susceptible to otherwise impermeable antibiotics and are resensitized to killing by last-resort antibiotics. This study supports FabH as a promising target for inhibition in future antimicrobial therapies.

KEYWORDS fatty acid biosynthesis, outer membrane permeability, antibiotic potentiation, multidrug resistance

Editor Paul M. Dunman, University of Rochester

Address correspondence to Yaoqin Hong, yaoqin.hong@qut.edu.au, or Makrina Totsika, makrina.totsika@qut.edu.au.

*Present address: Anthony D. Verderosa, Institute for Molecular Bioscience, University of Queensland, QLD 4072, Australia.

The authors declare no conflict of interest.

Received 25 February 2022
Accepted 24 March 2022
Published 16 May 2022

The outer membrane (OM) of Gram-negative bacteria is critical to their survival within harsh yet fluctuating environments (1). Unlike the canonical cytoplasmic membrane, the OM has an asymmetrical design, in which the inner leaflet is almost exclusively composed of phospholipids (PLs) while the outer leaflet is filled with the lipid A components of lipopolysaccharide (LPS) (2). Each LPS molecule carries anionic charges due to phosphate and carboxylate groups, which provides much of the OM rigidity through intermolecular interactions. The uniformly distributed LPS molecules on the outer leaflet of OM make it a potent barrier and guard the bacterium from harmful compounds (3). Moreover, each LPS molecule is capped by a hydrophilic core oligosaccharide, and in most cases, a terminal long-chain polysaccharide is also attached to the core oligosaccharide. In effect, this creates an additional stabilizing and protecting water-rich layer extending from the cell surface (4). For nutrient uptake, the otherwise impermeable OM houses a set of specialized porin proteins that allows solute exchange (3).

Over the past decades, the emergence of resistance to currently available antibiotics among many clinically important bacterial pathogens has been recognized as a major threat to global public health. In response to this challenge, the World Health Organization released a list of high-priority pathogens urgently requiring new antimicrobials (5, 6). Within the critical priority category of this list is the third-generation cephalosporin and/or carbapenem-resistant *Enterobacteriaceae* (including *Escherichia coli*, *Klebsiella*, *Serratia*, and *Proteus*). Many circulating pathogenic *E. coli* lineages are multidrug-resistant (MDR) and therefore remain susceptible to only a few available treatment options, which are fast diminishing (7, 8). One key contributor to antimicrobial resistance (AMR) in Gram-negative bacteria is their OM. Most effective antibiotics access their intracellular targets using OM-spanning hydrophilic porin channels, but this transport is restricted by both the chemical properties and the size of the permeant antibiotics. In the *Enterobacteriaceae* family, only small hydrophilic antibiotics ($<$600 kDa) can permeate the generalized porins (9, 10).

In bacteria, the essential acyl chains of PL and LPS are *de novo* synthesized by the highly conserved type II fatty acid synthesis pathway (FAS II) (11, 12). The structural heterogeneity of acyl chains present in membrane lipids can determine how bacteria respond to challenging and fluctuating environments (13–19). As seen in other essential pathways, FAS II has evolved specialized components, which possess overlapping biochemical activities and complex redundancies. Thus, several enzymes are redundant despite the essentiality of their biochemical activities. For example, in *E. coli*, three β-ketoacyl acyl carrier protein (ACP) synthases (KAS proteins)—FabB for KAS I activity (encoded by *fabB*), FabF for KAS II (encoded by *fabF*), and FabH for KAS III (encoded by *fabH*)—collectively take part in the Claisen condensation reactions to drive fatty acid (FA) biosynthesis (11). FabH initiates FA biosynthesis through condensing acetyl coenzyme A (CoA) with malonyl ACP (20), while FabB and FabF take overlapping roles in the subsequent polymerization steps (11). The associated substrate specificity has been reported in great detail by J. L. Garwin et al. (21).

The PL-LPS ratio, maintenance of membrane asymmetry, surface charge profiles of the surface exposed LPS, and chemical differences within both the PLs and LPS components collectively define the overall physicochemical and biological properties of the OM (22). As such, progress in understanding the OM may lead to valuable tactics to circumvent this formidable protective barrier and improve antibiotic cell entry in Gram-negative bacteria. In this work, we examined the role of redundant FAS II genes in maintaining the antimicrobial exclusion properties of the membrane barrier in clinically relevant uropathogenic *E. coli* (UPEC) strains, including a reference MDR isolate from the globally disseminated sequence type 131 (ST131) lineage (23, 24). We report that UPEC Δ*fabH* strains lacking KAS III activity display a severely defective membrane envelope and therefore are highly sensitive to antibiotic killing (up to 41-fold reduced MIC), even by otherwise ineffective drugs and while still harboring relevant AMR determinants. Moreover, this increased sensitivity held true in established biofilm eradication and the treatment of infected human bladder cell monolayers. Together, this work

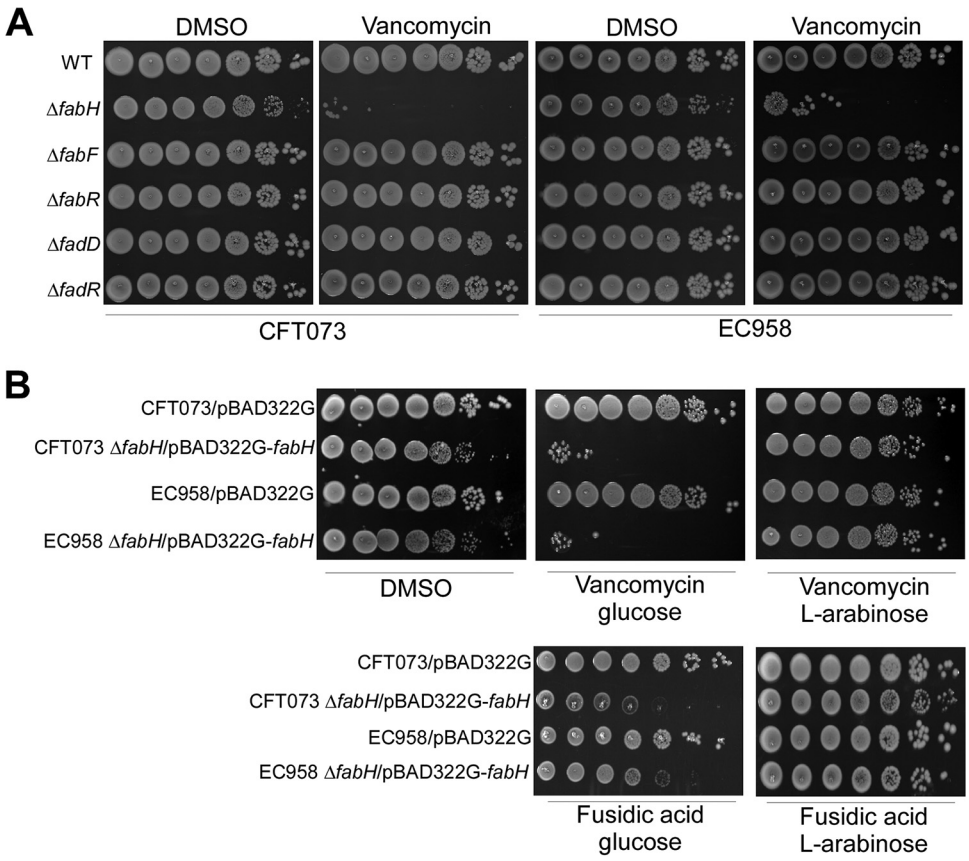

FIG 1 Screening UPEC FAS II mutants for membrane barrier defects using vancomycin. (A) CFT073 and EC958 WT and FAS II mutants were cultured on LB-Lennox agar containing 50 μg/mL vancomycin or DMSO carrier control. (B) Complementation of defective membrane barrier in CFT073 and EC958 Δ*fabH* using plasmid-borne *fabH* expressed under arabinose control. Overnight cultures normalized to an OD_{600} of 1.0 were serially diluted to 1E-6, and 5 μL of each dilution was spotted platted onto plates containing DMSO, 50 μg/mL vancomycin, or 100 μg/mL fusidic acid. Where appropriate, 1% D-glucose or 50 mM L-arabinose was supplemented to suppress or induce the expression of plasmid-encoded *fabH*, respectively. The plate images shown are representative of at least three independent experiments.

showcases FabH as a promising FAS II component that could be therapeutically targeted to rescue failing last-resort antibiotics and expand the range of currently available antibiotic treatments for Gram-negative infections.

RESULTS

***FabH* contributes to outer membrane barrier function in UPEC.** To study the involvement of the redundant genes in the FAS II pathway in the maintenance of the OM barrier, we used two model UPEC strains, CFT073 (a drug-sensitive reference pyelonephritis isolate) and EC958 (a reference MDR ST131 cystitis isolate), and constructed null mutants of the *fabH*, *fabF*, *fabR*, *fadR*, and *fadD* genes. Mutants were evaluated for OM defects by measuring their susceptibility to subinhibitory concentrations of vancomycin (25). UPEC Δ*fabF*, Δ*fabR*, Δ*fadR*, and Δ*fadD* mutants had growth similar to that of the wild type (WT) on LB-Lennox containing 50 μg/mL vancomycin, in both strains (Fig. 1). Like previous *E. coli* K-12 Δ*fabH* studies (26, 27), UPEC Δ*fabH* strains grew remarkably slower than the WT strains (Fig. S1), and this is reflected in the reduced colony size illustrated in Fig. 1A. Notably, despite the growth defect, the Δ*fabH* sample plated onto dimethyl sulfoxide (DMSO) carrier control plates contained a similar number of viable CFU as the optical density at 600 nm (OD_{600})-matched WT inoculum (Fig. 1A).

As expected, WT strains of EC958 and CFT073 survived low-dose vancomycin, a Gram-positive antibiotic that is normally ineffective against Gram-negative bacteria, as

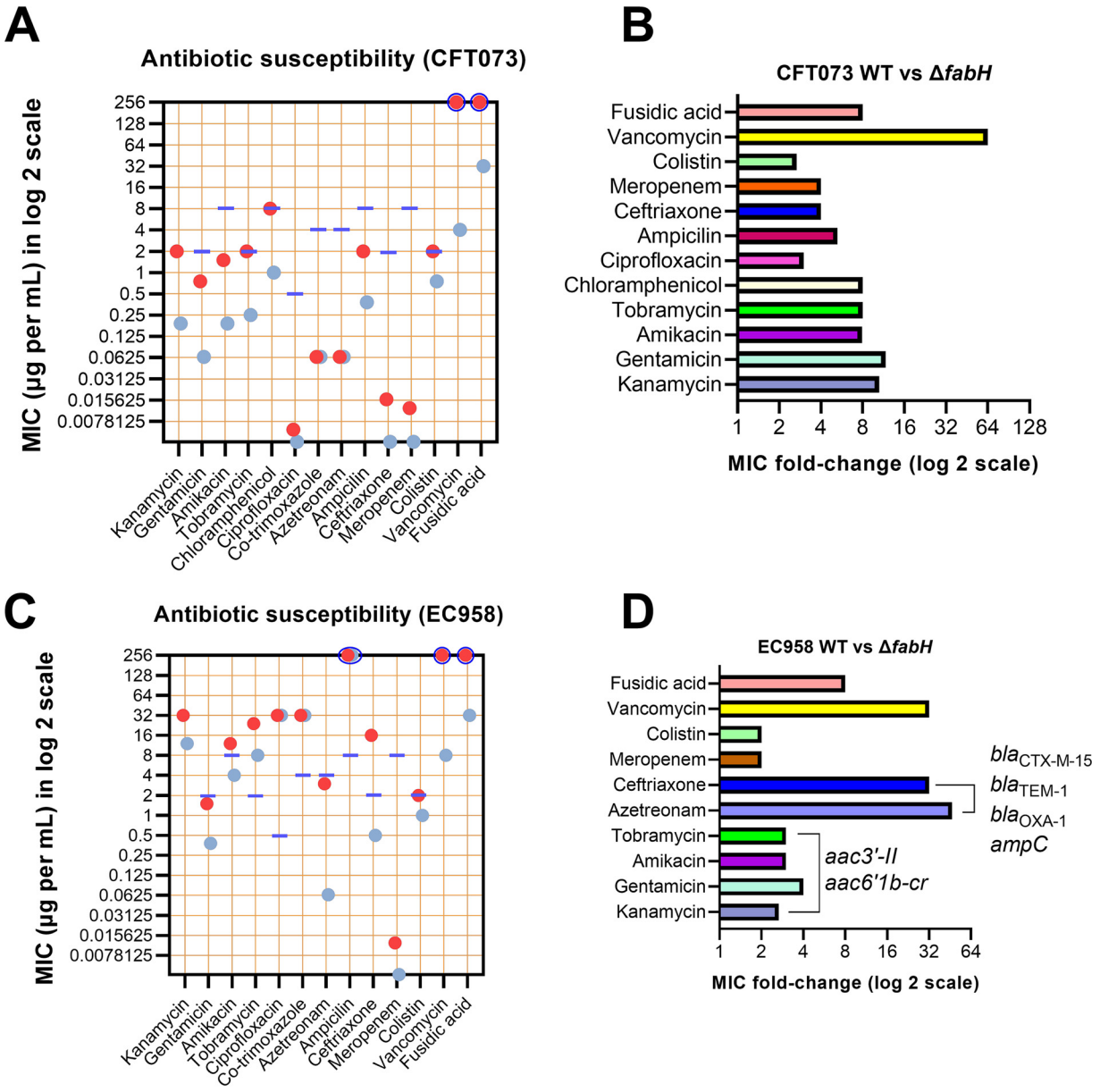

FIG 2 Loss of KAS III activity potentiates UPEC killing by a wide array of antibiotics. (A) Individual antibiotic MICs for CFT073 WT (red dots) and Δ*fabH* strains (blue dots). (B) Antibiotic MIC fold changes (improvement in potency) for the CFT073 Δ*fabH* mutant relative to the WT. (C) Individual antibiotic MICs for EC958 WT (red dots) and Δ*fabH* (blue dots). (D) Antibiotic MIC fold changes (improvement in potency) for the EC958 Δ*fabH* mutant relative to the WT. The purple lines in panels A and C mark current clinical resistance MIC cutoffs for each antibiotic as listed in the European Committee on Antimicrobial Susceptibility Testing tables (31). MIC values that exceeded the testing range of the Liofilchem MIC strips are indicated by blue circles that enclose the red/blue dot(s).

the OM prevents penetration to reach its peptidoglycan target. In contrast, CFU of the Δ*fabH* mutants were diminished by 5-logs when exposed to 50 μg/mL vancomycin (Fig. 1A). Likewise, we also observed similar increased sensitivity to fusidic acid, a hydrophobic antibiotic, which like vancomycin, is normally only effective against Gram-positive bacteria (Fig. 2B). We then introduced the *fabH* gene into the Δ*fabH* mutants on the low-copy-number and tightly controllable pBAD322G vector under P*ara* control (28). Intrinsic resistance to both vancomycin and fusidic acid was fully restored to WT levels upon induction of FabH expression, but not when transcription was catabolically repressed (Fig. 1B). We also noticed a similar susceptibility pattern in laboratory K-12 strains; thus, the cryptic OM of the Δ*fabH* strain is not restrictive to UPEC but generally applies to most, if not all, *E. coli* strains (data not shown).

Loss of *FabH* promotes UPEC killing by several antibiotics. We hypothesized that the defective OM allows the efficient penetration of antibiotics and potentiates their inhibitory effect. To assess this, we determined the MIC of Δ*fabH* strains to a wide range of antibiotics (Fig. 2 and Table S2). As expected, fusidic acid and vancomycin that cannot penetrate the Gram-negative cell envelope displayed an MIC of >256 μg mL^{-1} against CFT073 WT (Fig. 2A). In marked contrast, for CFT073 Δ*fabH*, the vancomycin MIC was reduced by >64-fold, whereas for fusidic acid, a >8-fold MIC reduction was observed (Fig. 2A and B). Antibiotics representing the β-lactam, aminoglycoside, phenicol, polymyxin, and quinolone/fluoroquinolone classes were also tested. A >8-fold increase in susceptibility to both aminoglycosides (kanamycin, gentamicin, amikacin, and tobramycin) and phenicol (chloramphenicol) was observed. Moreover, the MIC values of ceftriaxone, meropenem, colistin, and ciprofloxacin against the isogenic CFT073 Δ*fabH* mutant were further decreased by 2- to 4-fold (Fig. 2A and B), despite these antibiotics already being active at sub-μg per mL concentrations against the susceptible CFT073 strain. Interestingly, we found CFT073 to be phenotypically resistant to tobramycin, chloramphenicol, and colistin, although it lacks recognizable antibiotic-resistant determinants (29).

The restored susceptibility to three antibiotics (tobramycin, chloramphenicol, and colistin) in CFT073 Δ*fabH* prompted us to test if antibiotic efficacy could be restored against resistant strains. EC958 is an MDR clinical isolate of the globally disseminated ST131 lineage, carrying resistance genes to several antibiotic classes, including β-lactams ($bla_{\text{CTX-M-15}}$, $bla_{\text{TEM-1}}$, $bla_{\text{OXA-1}}$, bla_{CMY23}, and *ampC*), aminoglycosides (*aac3′-II* and *aac6′1b-cr*), and sulfonamides (*dhfrVII*, *aadA5*, and *sul1*), in addition to two chromosomal mutations (S83L and D87N mutations in the *gyrA* gene) that confer fluoroquinolone resistance (23, 24, 30).

We attributed the very high co-trimoxazole and ciprofloxacin MIC values (>32 μg/mL) of EC958 WT and Δ*fabH* to the sulfonamide and quinolone resistance determinants present in the strain (Fig. 2C). Like in CFT073, loss of *fabH* rendered EC958 susceptible to vancomycin (>32-fold change in MIC), fusidic acid (>8-fold), and colistin (2-fold) (Fig. 2D). Moreover, relative to the WT, EC958 Δ*fabH* was >2- to 4-fold more susceptible to all four tested aminoglycosides (note that for EC958 WT, the kanamycin MIC exceeded the test range of the MIC strip, so the reported fold change is likely an underestimate; Fig. 2C and D). Importantly, amikacin susceptibility was restored in the EC958 Δ*fabH* mutant (Fig. 2C and D), despite the presence of the aminoglycoside resistance genes (23, 30). We next compared the susceptibility of EC958 WT and Δ*fabH* strains to ampicillin, ceftriaxone, and aztreonam. As an extended-spectrum β-lactamase-positive (ESBL-positive) isolate, EC958 was found to be resistant to ceftriaxone (16 μg/mL) and nearly intermediate-resistant to aztreonam (3 μg/mL) (Fig. 2C). For EC958 Δ*fabH*, we observed enhanced susceptibility relative to the WT. The MIC values for ceftriaxone and aztreonam were reduced by 32-fold and ~47-fold, respectively (Fig. 2D). The extent of this MIC reduction rendered EC958 Δ*fabH* clinically susceptible to these otherwise ineffective antibiotics (with MICs well below the sensitivity values reported for *Enterobacterales* [31]).

The localization and folding of outer membrane proteins can be impacted by compositional changes in the bacterial membrane envelope (see recent review by J. E. Horne et al. [32] for detailed information). Therefore, in addition to the severed permeability barrier, efflux pumps may be impacted in Δ*fabH* and, as such, partially contribute to the observed antibiotic hypersensitivity. We probed the efflux activity of WT and Δ*fabH* strains of both CFT073 and EC958, using intracellularly accumulated ethidium bromide (Fig. 3). A Δ*tolC* mutant was constructed in EC958 as an efflux-defective control. As expected, ethidium bromide efflux was significantly delayed in this mutant (Fig. 3). In contrast, ethidium bromide was rapidly expelled from both the WT control and the Δ*fabH* mutant (Fig. 3). We conclude that efflux activity is unaffected in UPEC Δ*fabH* strains.

Loss of KAS III activity restores UPEC sensitivity to last-line carbapenems. Intriguingly, unlike other antibiotics of the β-lactam class, the Δ*fabH* strains were only twice more susceptible to meropenem than the WT strains (Fig. 2D). Both UPEC strains

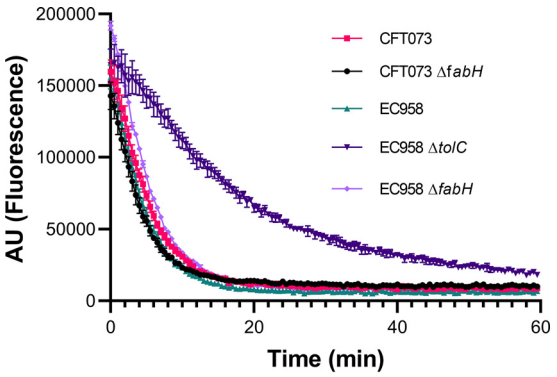

FIG 3 Efflux activity is unaffected in UPEC Δ*fabH* strains. Efflux kinetics of accumulated ethidium bromide were tracked in late-phase bacterial cultures by excitation at 525 nm and emission at 615 nm. Experiments were performed in biological triplicates, and average fluorescence readings (arbitrary units) taken every 30 s are plotted with error bars showing standard deviation (SD) values.

lack genes for carbapenem resistance, so we introduced a *kpc2*-containing plasmid (medium copy pSU2718 vector [33]) into the WT and Δ*fabH* strains to directly determine the impact of losing KAS III activity on carbapenem resistance.

Remarkably, the KPC-producing CFT073 Δ*fabH* strain displayed a reduced meropenem MIC by more than 21-fold relative to the WT strain (Fig. 4 and Table S3). Similarly pronounced results were observed for three other carbapenem antibiotics, with the MIC of imipenem, doripenem, and aztreonam reduced by 32-fold, >31-fold, and >42-fold, respectively (Fig. 4B and Table S3). All tested carbapenems (other than aztreonam) regained clinical potency against the KPC-producing UPEC Δ*fabH* strain. Overall, the loss of KAS III activity rendered the resistant parent strain remarkably susceptible to last-line carbapenems, with MIC values 4- to 10.5-fold lower than the current European Committee on Antimicrobial Susceptibility Testing resistance cutoff values for *Enterobacterales* (31).

Prompted by the enhanced vulnerability of Δ*fabH* strains to last-line β-lactams and considering the severe OM defects observed in the UPEC strains lacking KAS III activity, we hypothesized that periplasmic β-lactamases may escape from the cell through the

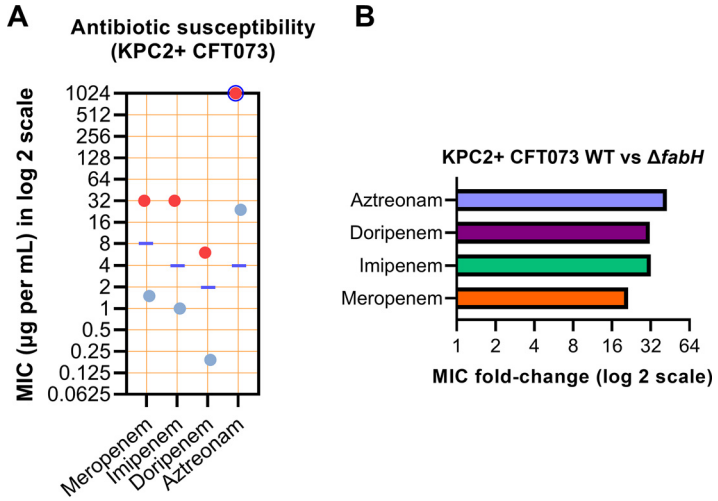

FIG 4 Carbapenemase-producing UPEC Δ*fabH* show restored susceptibility to carbapenem antibiotics. (A) MIC values for four carbapenem antibiotics tested against KPC-producing CFT073 WT (red dots) and isogenic Δ*fabH* (blue dots). The purple line indicates the latest current resistant MIC cutoff value for each antibiotic listed in the European Committee on Antimicrobial Susceptibility Testing tables (29). For MIC values that exceeded the testing range of the Liofilchem MIC strips, a blue circle is used to enclose the red/blue dot(s). (B) Carbapenem susceptibility MIC fold change (improvement in potency) for the KPC2+ CFT073 Δ*fabH* mutant relative to WT.

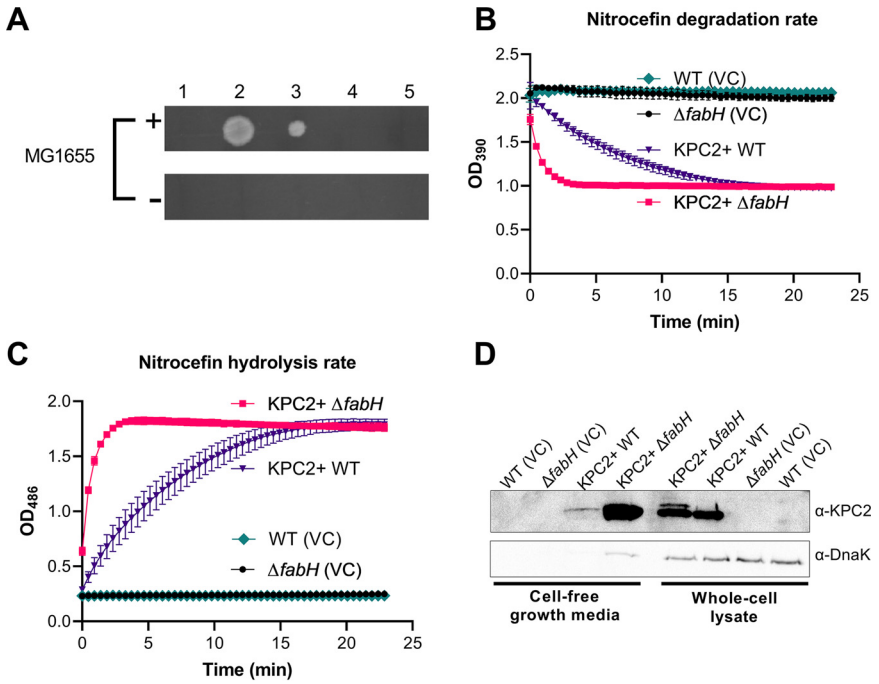

FIG 5 Evidence for leakage from the CFT073 Δ*fabH* severely compromised the outer membrane. (A) KPC2+ Δ*fabH* cell-free growth medium rescues MG1655 growth in meropenem-containing agar. (1) Growth medium harvested from KPC2+ WT; (2) growth medium harvested from KPC2+ Δ*fabH*; (3) heat-treated KPC2+ Δ*fabH* growth medium; (4) proteinase K-treated KPC2+ Δ*fabH* growth medium; (5) LB-Lennox medium control. Cell-free growth media were applied to meropenem plates swabbed with MG1655 (+) or no bacteria (–). (B) Nitrocefin degradation assays using cell-free growth media recovered from KPC2+ CFT073 WT and Δ*fabH*. (C) Nitrocefin hydrolysis assays using KPC2+ CFT073 WT and Δ*fabH* growth medium. (D) Western blot of KPC2 present in cell-free growth media and whole-cell preparations. Data from three biological replicates are shown in panels B and C as means ± SD. Images shown in panels A and D are representative of three biological replicates.

compromised OM, thereby reducing the periplasmic concentration of these protective enzymes in the previously resistant strain. To test this tenet, we collected cell-free media from the late log phase cultures of KPC2+ CFT073 WT and Δ*fabH* strains. Medium harvested from the KPC2+ Δ*fabH* culture, but not KPC2+ WT, rescued the growth of carbapenem-susceptible *E. coli* K-12 MG1655 on LB-Lennox agar containing 4 μg/mL meropenem (Fig. 5A). Proteinase K treatment of this growth medium reversed the growth rescue of MG1655. In contrast, heat treatment only marginally reduced the growth of MG1655 on meropenem LB-Lennox (Fig. 5A). This observation is consistent with the previously reported thermostability of KPC2 (34).

We next diluted cell-free culture media to assay β-lactamase activity with nitrocefin, a chromogenic cephalosporin substrate (Fig. 5B and C) (35). Growth medium harvested from KPC2+ Δ*fabH* exhibited significantly stronger β-lactamase activity than that of the KPC2+ WT (Fig. 5B and C). To confirm that KPC2 was present in significant amounts in the Δ*fabH* cell-free culture medium, proteins from the supernatant were concentrated and analyzed by Western blotting using anti-KPC2 antisera. As expected, we detected KPC2 in whole-cell lysates of KPC2+ CFT073 but not in the vector control (Fig. 5D). KPC2+ CFT073 Δ*fabH* had amounts of KPC2 comparable to those of the WT, although an additional higher-molecular-weight band consistent with premature KPC2 was also detected (Fig. 5D).

In the cell-free culture supernatant fraction, we detected a weak signal for KPC2 in the KPC2+ CFT073 sample (Fig. 5D). In striking contrast, very large amounts of KPC2 were observed in the KPC2+ Δ*fabH* culture medium sample (Fig. 5D). A weak band corresponding to the cytoplasmic chaperone protein DnaK was also detected, indicating minor levels of cell lysis (Fig. 5D). However, based on the very high KPC2:DnaK ratio

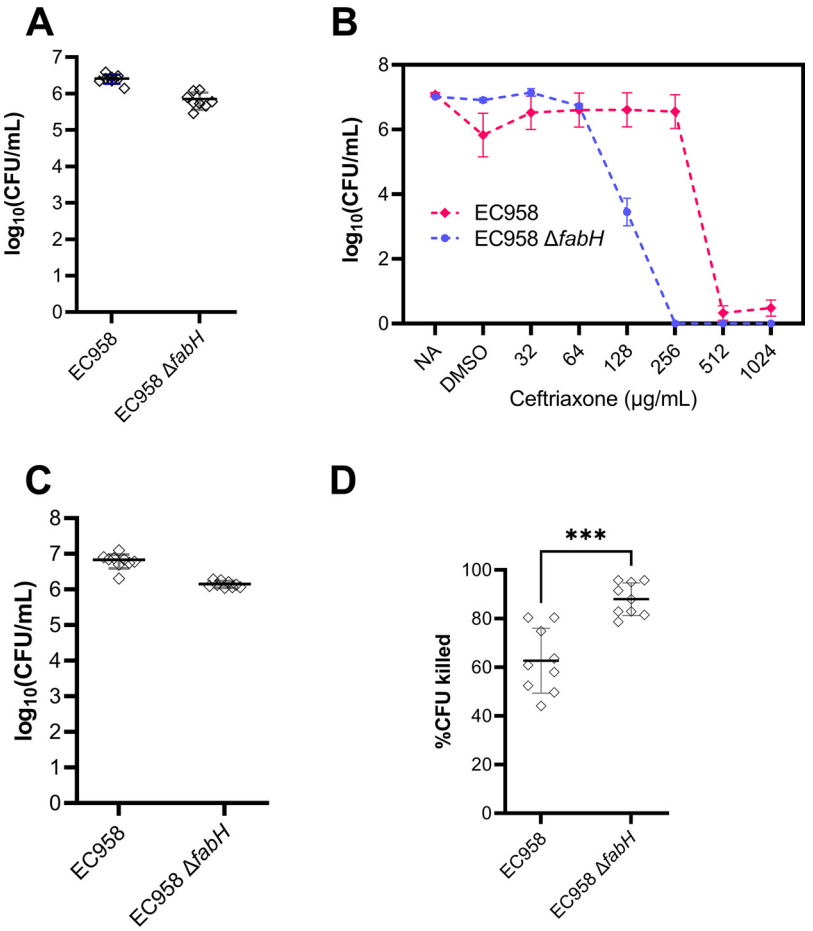

FIG 6 Preclinical evaluation of KAS III as a target aiding the eradication of UPEC biofilms and treatment of human bladder cell infection with antibiotics. (A) EC958 WT and Δ*fabH* establish mature biofilms of comparable biofilm on the Calgary biofilm device; (B) Ceftriaxone MBEC assessment of EC958 WT and Δ*fabH* biofilms, including untreated (NA) and drug carrier (DMSO) controls. (C) Total adherent bacteria on T24 bladder cell monolayers infected for 24 h at an MOI of 10 with EC958 WT and Δ*fabH*. (D) Reduction in viable CFU recovered from UPEC-infected T24 monolayers following a 1-h treatment with ceftriaxone (8 μg/mL). Group means were compared by an unpaired *t* test (***, $P = 0.003$).

in the sample compared to that of the whole cell (Fig. 5D), we reasoned that the bulk of KPC2 detected in the cell supernatant likely escaped to the extracellular milieu through the severely compromised OM of Δ*fabH* intact cells.

Loss of KAS III activity potentiates ceftriaxone treatment of ESBL+ UPEC biofilms and infected human bladder cells. UPEC bacteria form biofilms on biotic and abiotic surfaces that are recalcitrant to antibiotic treatment and aid bacterial survival inside bladder cells and on urinary catheters (36, 37). To investigate whether the enhanced antibiotic susceptibility of UPEC Δ*fabH* strains observed in planktonic drug sensitivity assays can be extended to improved activity against established biofilms, we grew EC958 WT and Δ*fabH* mature biofilms with both strains establishing comparable viable biofilm cell densities after 24 h (Fig. 6A). While biofilms formed by either strain had very high ceftriaxone resistance, a 4-fold reduction in the minimal biofilm eradication concentration (MBEC) was observed for Δ*fabH*, with a ceftriaxone MBEC of 512 μg/mL for the WT and 128 μg/mL for Δ*fabH* (Fig. 6B). Interestingly, residual EC958 WT cells remained viable even at the highest ceftriaxone dose tested (1,024 μg/mL), while no viable Δ*fabH* cells were detected in biofilms treated at and above 256 μg/mL ceftriaxone, i.e., achieving complete biofilm eradication (Fig. 6B).

We next tested if ceftriaxone is effective in treating established human cell infection by EC958—a strain that is clinically resistant to this antibiotic. Infection of

human T24 bladder cell monolayers with EC958 WT and Δ*fabH* at a multiplicity of infection (MOI) of 10 resulted in high-level adhesion ($>10^6$ CFU per monolayer) by both strains, albeit at slightly lower levels for Δ*fabH* (Fig. 6C). Subsequent 1-h treatment of infected monolayers with 8 μg/mL ceftriaxone eliminated ~90% of Δ*fabH* from the monolayer, while only a <65% reduction was observed for the WT (Fig. 6D). Taken together, our preclinical data on improved antibiotic activity against resistant *E. coli* in planktonic, biofilm, and cell infection models support the tenet that FabH constitutes a promising antimicrobial target for reviving failing last-resort antibiotics.

DISCUSSION

AMR is one of the top 10 global public health threats of the 21st century, and tackling this invisible pandemic constitutes a current priority (38–40). A recent report highlights that 1.27 million deaths in 2019 were directly attributable to resistant bacterial infections, with *E. coli* being the leading cause (6). Tactics to extend the life of existing antimicrobial agents or expand their spectrum are becoming a necessity in light of the dwindling antibiotic discovery pipeline, as new antibiotics are sparse. As an evolving permeability barrier, the OM is instrumental in developing antibiotic resistance in Gram-negative bacteria (9, 41). In recent years, there has been a resurgence of interest in exploring the disruption of the OM as an antimicrobial tactic (42–45). FAs are the common building blocks for structural lipids in the cytoplasmic membrane and the OM; thus, their biosynthetic pathways present attractive antibiotic targets (46). Here, we showed that the loss of KAS III incapacitates the OM to drastically improve antibiotic activity against clinical *E. coli*, even in the presence of acquired antibiotic resistance determinants.

Carbapenem is one of the last-resort antibiotics used to treat infections caused by drug-resistant Gram-negative bacterial infections. Unfortunately, resistance to carbapenems is increasingly prevalent in *E. coli* and other members of the *Enterobacteriaceae* family (47). We showed that targeting FabH can deactivate the antibiotic protection offered by advanced β-lactamases and carbapenemase to clinical *E. coli* strains. Another attractive prospect of targeting FabH (or other similar membrane perturbation tactics), is expanding the range of drugs with physicochemical properties amenable to Gram-negative entry, potentially expanding the spectrum of activity of many Gram-positive antibiotics.

FabH was previously thought to be indispensable in *E. coli* (48). However, this essentiality is bypassed by the product of the *yiiD* gene (renamed MadA) (49). The bypass mechanism involves the decarboxylation of malonyl ACP to produce acetyl ACP (50). Unlike acetyl-CoA, which can only be integrated into the initiation step of FA biosynthesis by FabH, this substrate can be used by FabB/FabF to bypass the loss of KAS III activity in *E. coli* (50). However, the supply of FA to integrate into membrane biogenesis by the MadA bypass is highly restrictive, and as such, earlier *E. coli* K-12 studies reported that Δ*fabH* cells are tiny (26, 27). This observation had been instrumental in developing the lipid-centric view that FA availability sets the capacity of the cell envelope to dictate cell size (27). Intriguingly, both CFT073 and EC958 Δ*fabH* cells have comparable size to their corresponding WT cells, though at the expense of cell division rate (Fig. S2). Together, these findings suggest that an additional layer of regulation might be employed in the two UPEC strains, allowing them to reach a destined cell envelope capacity despite severe FA starvation. Nonetheless, we note that antibiotic potentiation of Δ*fabH* is unrelated to cell size, given that K-12 Δ*fabH* cells with reduced size also displayed increased sensitivity to hydrophobic antibiotics (26), and we also observed a 42-fold and 6-fold potentiation to vancomycin and fusidic acid in K-12 strains lacking KAS III (data not shown).

Two recent studies had linked FA starvation to increased antibiotic tolerance (51, 52). Sublethal inhibition of FA biosynthesis either by blocking the chain elongation steps catalyzed by FabB/FabF or the enoyl ACP reductase FabI activates the

(p)ppGpp synthetase, RelA, which overproduces ppGpp, the effector molecule of stringent bacterial response (51, 52). A high ppGpp level inadvertently drives *E. coli* and several other species to reach an antibiotic-tolerant state (51–57). The loss of KAS III also triggers the overproduction of ppGpp (26). In fact, the production of the stringent response alarmone is necessary for the survival of Δ*fabH*, as ppGpp is required to drive the transcription of MadA that partially substitutes FabH (49). Yet, in multiple *E. coli* lineages, Δ*fabH* shows hypersensitivity toward a broad panel of antibiotics.

Yao et al. (26) reported that the membrane lipids of Δ*fabH* contain elevated ratios of unsaturated fatty acids. We expected the cytoplasmic membrane would also be altered in a Δ*fabH* strain. However, In the context of drug diffusion, influx across the cytoplasmic membrane, composed of phospholipids, is orders of magnitude faster than flux across the outer membrane. As such, drug diffusion across the outer membrane is the key rate-limiting step to achieve antibiotic potentiation. Given the extent to which the cell envelope is disrupted in Δ*fabH*, presumably allowing leakage of large periplasmic contents (Fig. 5D), this damage alone is sufficient to overcome antibiotic tolerance induced by the stringent response. Nonetheless, to our surprise, the strain that possessed such a cryptic cell envelope remained highly stable, demonstrated by our failed previous attempts to isolate the then unresolved functional bypass of KAS III activity through permissive conditions (Hong Y and Cronan JE, unpublished). The mystery may lie in the multifaceted network regulating FAS II (58, 59) and other related pathways to compensate for defects in membrane biogenesis (60).

MATERIALS AND METHODS

Bacterial strains and growth. The strains and plasmids used in this study are described in Table 1. The *E. coli* strains were grown at 37°C in lysogeny broth (LB)-Lennox unless otherwise indicated. For solid media, 15 g/L bacteriological agar was added. Ampicillin was used at 100 μg/mL, chloramphenicol at 17 μg/mL, and gentamicin at 10 μg/mL.

Cloning and genetic manipulations. The *fabH* gene was amplified from the genomic DNA of the K-12 strain MG1655 and cloned into the BamHI and PstI sites in the pBAD322G vector (28). pKPC2 was constructed by amplifying Tn*4401a-kpc2* from the genomic DNA of a clinical *K. pneumoniae* strain, JIE2709 (61), and cloned into the PstI and KpnI sites in pSU2718 (33). Lambda recombination competency was achieved by adding temperature-sensitive plasmids, either pKD46 (62) or pKOBERG-Gen (63), to the manipulating strain. Transformation and lambda recombination were performed as previously described (64). Temperature-sensitive pCP20-Gent carrying FLP recombinase was used to remove the *cat* marker wherever applicable. For the construction of EC958 Δ*tolC*::*cat*, lambda-red recovery culture postelectrotransformation was platted onto a low-dose chloramphenicol (6.5 μg/mL chloramphenicol) LB-Lennox plate and isolated and screened from a thin bacterial lawn. Oligonucleotide sequences used for gene replacements and cloning are included in Table S1.

Outer membrane defect assay. Vancomycin can only transverses the Gram-negative OM when the permeability barrier is compromised (65). The OM defect of the null mutants constructed was assayed using susceptibility of a dilution series from overnight-grown cultures adjusted to an OD_{600} of 1.0 to subinhibitory concentrations of vancomycin similar to the method previously described (66, 67). Equivalent loading of the OD_{600}-adjusted samples (5 μL) was spot-plated onto LB agar.

Ethidium bromide efflux assay. Stationary cultures were diluted with fresh LB-Lennox containing 1 mg/L ethidium bromide and 20 μg/mL carbonyl cyanide *m*-chlorophenylhydrazone. Cultures were incubated at 37°C until an OD_{600} of 0.7 to 0.8 was reached with aeration. The cells pellets were harvested via centrifugation and washed with 4× volumes of 1× phosphate-buffered saline (PBS). The samples were then resuspended in 1× PBS and incubated for 30 min in a dark room at 5°C. The samples were adjusted to an OD_{600} of 0.2 and dispensed in 150-μL volumes in a Greiner 96-well flat-bottom plate; D-glucose (20% wt/vol stock) was then added at a 0.1% concentration (12 μL) to energize ethidium bromide efflux. Efflux activity was tracked over 60 min in a CLARIOStar instrument (BMG, Australia) at 37°C. The following instrumental settings were used: excitation at 525 ± 15, emission at 615 ± 20, auto 568.8 dichroic filter. The experiment was performed in biological triplicates.

Determination of antibiotic MICs. The specific bacterial strains were prepared and tested according to the MIC test strips (Liofilchem) manufacturer's instructions. Briefly, overnight cultures of the specific strains were diluted in 0.85% (wt/vol) saline to give a final inoculum concentration of 1.5×10^8 CFU mL^{-1}. The inoculums were then used to inoculate Mueller-Hinton agar (Thermo Fisher, Australia) plates using a sterile swab. The MIC test strip was applied to the agar surface after the inoculum had dried. Plates were then incubated at 37°C for 20 h. The MIC values were determined by observing where the relevant inhibition ellipse intersected with the MIC test strip.

TABLE 1 Strains and plasmids used in this work

Strains and plasmids	Detail	Source or reference
Strains		
MG1655	*E. coli* K-12 strain; F-λ-*ilvG rfb-50 rph-1*	Coli Genetic Stock Centre
MT1776	MG1655 Δ*fabH*::*cat*	This work
CFT073	Pyelonephritogenic *E. coli* isolate (O6:K2:H1)	69
MT2099	CFT073/pBAD322G	This work
MT1534	CFT073 Δ*fabH*::*FRT*	This work
MT2092	CFT073 Δ*fabH*::*FRT*/pBAD322G-*fabH*	This work
MT534	CFT073 Δ*fabR*::*cat*	This work
MT1427	CFT073 Δ*fadR*::*cat*	This work
MT1439	CFT073 Δ*fadD*::*cat*	This work
MT1496	CFT073 Δ*fabF*::*FRT*	This work
MT1803	CFT073/pKPC2	This work
MT1804	CFT073 Δ*fabH*::*FRT*/pKPC2	This work
EC958	*E. coli* ST131 urinary tract infection isolate (O25b:H4), MDR	23
MT2098	EC958/pBAD322G	This work
MT1667	EC958 Δ*fabH*::*cat*	This work
MT2100	EC958 Δ*fabH*::*cat*/pBAD322G-*fabH*	This work
MT1901	EC958 Δ*fabR*::*cat*	This work
MT1902	EC958 Δ*fabF*::*cat*	This work
MT1903	EC958 Δ*fadD*::*cat*	This work
MT1917	EC958 Δ*fadR*::*cat*	This work
MT1608	EC958 Δ*tolC*::*cat*	This work
Plasmids		
pKPC2	Tn-4401a-*kpc2* cloned into pSU2718, chloramphenicol resistance	This work
pBAD322G	*araBAD* promoter-based expression vector, complete pBR322 origin, gentamicin resistance	28
pSU2718	p15A-derived plasmids carry *lacZ*α reporter gene, chloramphenicol resistance	33
pBAD322G-*fabH*	K-12 MG1655 *fabH* cloned into the BamHI/PstI sites of pBAD322G	This work
pKD3	FRT-flanked cat gene, oriRγ replicon, ampicillin, and chloramphenicol resistance	62
pKD46	λ recombineering genes (α, β, γ) controlled by arabinose-inducible promoter, P*araB*, temp-sensitive oriR101 replicon, ampicillin resistance	62
pCP20	*flp* recombinase gene, temp-sensitive replicon, ampicillin, and chloramphenicol resistance	62
pKOBERG-Gen	Gentamicin-resistant plasmid carrying the λ recombineering genes (α, β, γ)	70

Determination of carbapenemase activity in cell-free growth media using MG1655 rescue. MT1803 and MT1804 overnight early stationary cultures were diluted 1:50 into fresh LB-Lennox containing chloramphenicol (17 μg/mL) and grown to an OD_{600} of 0.8 at 37°C. Cell-free growth media were prepared by the filtration of culture supernatant of OD_{600} 0.8 cultures grown at 37°C with aeration through a 0.22-μm filter (3M). The samples (5 μL) were spotted onto LB-Lennox agar containing meropenem (4 μg/mL) and had been swabbed with overnight cultures of MG1655 on the plate surface. Cell-free growth media treated with proteinase K at 37°C for 30 min and heat-treated (60°C for 30 min) cell-free growth media were also added to MG1655-swabbed LB-Lennox containing meropenem (4 μg/mL) to serve as controls. LB-Lennox containing meropenem (4 μg/mL) without MG1655 swab was also included as a control for the cell-free growth media. Plates were incubated at 37°C for 20 h, and images were taken with a Bio-Rad GelDocXR+ system using Image Lab software (v5.1; Bio-Rad). Figure 5D is representative of three biological replicates.

Assaying carbapenemase activity from cell-free growth media. MT1803 and MT1804 overnight early stationary cultures were diluted 1:50 into fresh LB-Lennox containing chloramphenicol (17 μg/mL) and grown to an OD_{600} of 0.8 at 37°C. The cell-free growth medium was prepared by filtering culture supernatant through a 0.22-μm filter (3MM). The cell-free growth media were then diluted 1:1,000 (180 μL) and adjusted to 150 μM nitrocefin to give a testing volume of 200 μL. Nitrocefin degradation assays using cell-free growth media recovered from KPC2+ CFT073 WT and Δ*fabH* were then performed using KPC2+ CFT073 WT and Δ*fabH* growth medium, with two variables, degradation of nitrocefin and generation of products tracked at 390 nm and 486 nm, respectively, on a CLARIOStar instrument (BMG, Australia) over time. Nitrocefin working stock was prepared at 1.5 mM in 50 mM phosphate buffer.

Precipitation of extracellular proteins and Western blot analysis. First, 5 mL of cell-free growth medium was prepared by the filtration of culture supernatant of OD_{600} 0.8 cultures grown at 37°C with aeration through a 0.22 μm filter (3MM). The sample was then precipitated with 1 mL of ice-cold 100% (wt/vol) trichloroacetic acid and incubated on ice for 10 min. The precipitated protein was harvested via centrifugation (20,000 × *g*, 4°C, 10 min), washed once with 500 μL of ice-cold acetone, and dissolved in 100 μL of SDS-PAGE sample buffer, with the pH adjusted with 1 M Tris-HCl, pH 9. Precipitated extracellular protein samples (10 μL) and whole-cell lysates (10 μL, derived from a 10× concentrate of OD_{600} 1.0

culture harvested simultaneously as cell-free growth media) were separated on 12% SDS-PAGE. The samples were transferred to nitrocellulose membranes. Immunoblot analyses were performed with rabbit α-KPC2 (1:8,000) and mouse α-DnaK (1:10,000; Enzo Life Sciences, kindly gifted by Renato Morona), followed by goat α-rabbit Amersham ECL HRP-conjugated antibodies (1:20,000; Cytiva) for chemiluminescent detection using Pierce ECL Western blot substrate. Rabbit polyclonal α-KPC2 sera were raised by inoculation with three previously described KPC2 peptide epitopes (epitope A: CFAKLEQDFGGSIGVYA; epitope B: CLNSAIPGDARDTSSPRAVT; epitope C: CVIAAAARLALEGLGVN [68]) at the Walter and Eliza Hall Institute of Medical Research (peptides were synthesized by Mimotopes Pty. Ltd.). The developed blots were imaged in the Bio-Rad GelDocXR+ system using Image Lab software (v5.1; Bio-Rad).

Biofilm growth. Minimum biofilm eradication concentration (MBEC) and biofilm growth assays were performed in a Calgary biofilm device (CBD) (MBEC assay; Innovotech, Inc., Canada). Overnight bacterial cultures in LB were diluted to 10^6 CFU/mL and used to inoculate the plate with 130 μL of culture per well. The CBD was incubated for 24 h with shaking (150 rpm) at 37°C in 95% relative humidity. Following 24 h of growth, biofilms were washed once in PBS to remove nonadherent cells and then sonicated for 20 min at 20°C. At least three biological and two technical repeats per strain per experiment were serially diluted and spotted onto LB agar plates to determine viable CFU recovered from each peg biofilm. Plates were incubated overnight at 37°C, and colonies were counted the following day to obtain $\log_{10}$ (CFU/mL) values for each strain.

MBEC assays. Following 24 h of biofilm growth in the CBD, biofilms were washed once in PBS to remove nonadherent cells, and the biofilm peg lid was transferred to a treatment plate containing various concentrations of ceftriaxone disodium salt heptahydrate or dimethyl sulfoxide (DMSO) in Muller Hinton broth. Peg biofilms were incubated in the treatment plate for 24 h and then sonicated and plated as per the biofilm growth assay. MBEC values were defined as concentrations with over 3 $\log_{10}$ reduction in CFU/mL.

Epithelial cell infection assay and ceftriaxone treatment. Intestinal epithelial T24 cells (ATCC HTB4; Dulbecco's modified Eagle's medium [DMEM]) were maintained in McCoy medium (Invitrogen) supplemented with 5% heat-inactivated fetal calf serum (Invitrogen). Bacterial strains were cultured under type 1 fimbria enrichment conditions, as previously described (23). Infection assays were performed as previously described (63). Briefly, confluent cell monolayers were infected with strains at a multiplicity of infection (MOI) of 10 and incubated at 37°C, 5% CO_2, for 1 h. PBS washes (3×) were used to remove nonadherent bacteria. Ceftriaxone salt heptahydrate (in DMSO) was added to McCoy medium and applied to the infected monolayer without disturbance. Antibiotic treatment was performed by incubation at 37°C, 5% CO_2, for 2 h. Then, 1× PBS washes (3×) were used to remove nonadherent bacteria and antibiotic residue. Monolayers were lysed with 0.1% (vol/vol) Triton X-100, and lysates were serially diluted and plated onto LB agar to enumerate total adherent bacteria.

SUPPLEMENTAL MATERIAL

Supplemental material is available online only.

FIG S1, TIF file, 0.6 MB.

FIG S2, TIF file, 0.2 MB.

FIG S3, TIF file, 1.3 MB.

TABLE S1, DOCX file, 0.01 MB.

TABLE S2, DOCX file, 0.01 MB.

TABLE S3, DOCX file, 0.01 MB.

ACKNOWLEDGMENTS

The rabbit α-EcDnaK was a generous gift from Renato Morona (University of Adelaide, Australia).

This work was supported in part by an Australian National Health and Medical Research Council Project grant (GNT1144046), a Clive and Vera Ramaciotti Health Investment grant (2017HIG0119), the Australian Research Council (DE130101169), a Georgina Sweet Award for Women in Quantitative Biomedical Science to M.T., and an Early Career Research Grant from the Institute of Health and Biomedical Innovations at the Queensland University of Technology, Australia, to Y.H. The CLARIOStar high-performance microplate reader (BMG, Australia) was sponsored by the Ian Potter Foundation. S.H. is the recipient of an Australian Government Research Training Program (RTP) Scholarship. B.Z. was supported by a China Scholarship Council (CSC) scholarship. M.T. received support from Queensland University of Technology through a Vice-Chancellor's Research Fellowship.

Y.H., J.E.C., and M.T. contributed to project conception; Y.H., J.Q., and M.T. contributed to experimental design. Y.H., J.Q., A.D.V., S.H., and B.Z. conducted experiments, data collection, analysis, and interpretation; Y.H. and M.T. supervised the study and obtained

the funding. Y.H. drafted the initial manuscript. Y.H. and M.T. substantially revised the manuscript. J.E.C. and M.A.T.B. contributed to data interpretation and revised the manuscript. All authors approved the final manuscript.

REFERENCES

1. Nikaido H. 1994. Prevention of drug access to bacterial targets: permeability barriers and active efflux. Science 264:382–388. https://doi.org/10.1126/science.8153625.
2. Cronan JE Jr. 1979. Phospholipid synthesis and assembly, p 35–65. *In* Inouye M (ed), Bacterial outer membranes. John Wiley, New York, NY.
3. Nikaido H. 2011. To the happy few. Annu Rev Microbiol 65:1–18. https://doi.org/10.1146/annurev-micro-090110-102920.
4. Reeves P, Cunneen MM. 2009. Biosynthesis of O-antigen chains and assembly, p 319–335. *In* Moran AP, Holst O, Brennan PJ, von Itzstein M (ed), Microbial glycobiology: structures, relevance and applications. Elsevier, Amsterdam, The Netherlands.
5. WHO. 2017. WHO global priority list of antibiotic-resistant bacteria to guide research, discovery, and development of new antibiotics. World Health Organization, Geneva, Switzerland.
6. Murray CJL, Ikuta KS, Sharara F, Swetschinski L, Robles Aguilar G, Gray A, Han C, Bisignano C, Rao P, Wool E, Johnson SC, Browne AJ, Chipeta MG, Fell F, Hackett S, Haines-Woodhouse G, Kashef Hamadani BH, Kumaran EAP, McManigal B, Agarwal R, Akech S, Albertson S, Amuasi J, Andrews J, Aravkin A, Ashley E, Bailey F, Baker S, Basnyat B, Bekker A, Bender R, Bethou A, Bielicki J, Boonkasidecha S, Bukosia J, Carvalheiro C, Castañeda-Orjuela C, Chansamouth V, Chaurasia S, Chiurchiù S, Chowdhury F, Cook AJ, Cooper B, Cressey TR, Criollo-Mora E, Cunningham M, Darboe S, Day NPJ, De Luca M, Dokova K, et al. 2022. Global burden of bacterial antimicrobial resistance in 2019: a systematic analysis. Lancet 399:629–655. https://doi.org/10.1016/S0140-6736(21)02724-0.
7. Asadi Karam MR, Habibi M, Bouzari S. 2019. Urinary tract infection: pathogenicity, antibiotic resistance and development of effective vaccines against uropathogenic Escherichia coli. Mol Immunol 108:56–67. https://doi.org/10.1016/j.molimm.2019.02.007.
8. McGann P, Snesrud E, Maybank R, Corey B, Ong AC, Clifford R, Hinkle M, Whitman T, Lesho E, Schaecher KE. 2016. Escherichia coli harboring mcr-1 and blaCTX-M on a novel IncF plasmid: first report of mcr-1 in the United States. Antimicrob Agents Chemother 60:4420–4421. https://doi.org/10.1128/AAC.01103-16.
9. Nikaido H. 2003. Molecular basis of bacterial outer membrane permeability revisited. Microbiol Mol Biol Rev 67:593–656. https://doi.org/10.1128/MMBR.67.4.593-656.2003.
10. Delcour AH. 2009. Outer membrane permeability and antibiotic resistance. Biochim Biophys Acta 1794:808–816. https://doi.org/10.1016/j.bbapap.2008.11.005.
11. Cronan JE Jr., Rock CO. 2008. Biosynthesis of membrane lipids. EcoSal Plus 3. https://doi.org/10.1128/ecosalplus.3.6.4.
12. Bertani B, Ruiz N. 2018. Function and biogenesis of lipopolysaccharides. EcoSal Plus 8. https://doi.org/10.1128/ecosalplus.ESP-0001-2018.
13. Cronan JE Jr. 1975. Thermal regulation of the membrane lipid composition of Escherichia coli. Evidence for the direct control of fatty acid synthesis. J Biol Chem 250:7074–7077. https://doi.org/10.1016/S0021-9258(19)41040-5.
14. Morein S, Andersson A-S, Rilfors L, Lindblom G. 1996. Wild-type Escherichia coli cells regulate the membrane lipid composition in a "window" between gel and non-lamellar structures. J Biol Chem 271:6801–6809. https://doi.org/10.1074/jbc.271.12.6801.
15. de Mendoza D, Cronan JE Jr. 1983. Thermal regulation of membrane lipid fluidity in bacteria. Trends Biochem Sci 8:49–52. https://doi.org/10.1016/0968-0004(83)90388-2.
16. Dong H, Cronan JE. 2021. Temperature regulation of membrane composition in the Firmicute, Enterococcus faecalis, parallels that of Escherichia coli. Environ Microbiol 23:2683–2691. https://doi.org/10.1111/1462-2920.15512.
17. Adams FG, Trappetti C, Waters JK, Zang M, Brazel EB, Paton JC, Snel MF, Eijkelkamp BA. 2021. To make or take: bacterial lipid homeostasis during infection. mBio 12:e0092821. https://doi.org/10.1128/mBio.00928-21.
18. Hassan N, Anesio AM, Rafiq M, Holtvoeth J, Bull I, Haleem A, Shah AA, Hasan F. 2020. Temperature driven membrane lipid adaptation in glacial psychrophilic bacteria. Front Microbiol 11:824. https://doi.org/10.3389/fmicb.2020.00824.
19. Xu Y, Zhao Z, Tong W, Ding Y, Liu B, Shi Y, Wang J, Sun S, Liu M, Wang Y, Qi Q, Xian M, Zhao G. 2020. An acid-tolerance response system protecting exponentially growing Escherichia coli. Nat Commun 11:1496. https://doi.org/10.1038/s41467-020-15350-5.
20. Heath RJ, Rock CO. 1995. Regulation of malonyl-CoA metabolism by acyl-acyl carrier protein and β-ketoacyl-acyl carrier protein synthases in Escherichia coli. J Biol Chem 270:15531–15538. https://doi.org/10.1074/jbc.270.26.15531.
21. Garwin JL, Klages AL, Cronan JE Jr. 1980. Beta-ketoacyl-acyl carrier protein synthase II of Escherichia coli. Evidence for function in the thermal regulation of fatty acid synthesis. J Biological Chemistry 255:3263–3265. https://doi.org/10.1016/S0021-9258(19)85692-2.
22. Paulowski L, Donoghue A, Nehls C, Groth S, Koistinen M, Hagge SO, Böhling A, Winterhalter M, Gutsmann T. 2020. The beauty of asymmetric membranes: reconstitution of the outer membrane of Gram-negative bacteria. Front Cell Dev Biol 8:586–586. https://doi.org/10.3389/fcell.2020.00586.
23. Totsika M, Beatson SA, Sarkar S, Phan MD, Petty NK, Bachmann N, Szubert M, Sidjabat HE, Paterson DL, Upton M, Schembri MA. 2011. Insights into a multidrug resistant Escherichia coli pathogen of the globally disseminated ST131 lineage: genome analysis and virulence mechanisms. PLoS One 6:e26578. https://doi.org/10.1371/journal.pone.0026578.
24. Petty NK, Ben Zakour NL, Stanton-Cook M, Skippington E, Totsika M, Forde BM, Phan MD, Gomes Moriel D, Peters KM, Davies M, Rogers BA, Dougan G, Rodriguez-Bano J, Pascual A, Pitout JD, Upton M, Paterson DL, Walsh TR, Schembri MA, Beatson SA. 2014. Global dissemination of a multidrug resistant Escherichia coli clone. Proc Natl Acad Sci U S A 111:5694–5699. https://doi.org/10.1073/pnas.1322678111.
25. Krishnamoorthy G, Wolloscheck D, Weeks JW, Croft C, Rybenkov VV, Zgurskaya HI. 2016. Breaking the permeability barrier of Escherichia coli by controlled hyperporination of the outer membrane. Antimicrob Agents Chemother 60:7372–7381. https://doi.org/10.1128/AAC.01882-16.
26. Yao Z, Davis RM, Kishony R, Kahne D, Ruiz N. 2012. Regulation of cell size in response to nutrient availability by fatty acid biosynthesis in Escherichia coli. Proc Natl Acad Sci U S A 109:E2561–E2568. https://doi.org/10.1073/pnas.1209742109.
27. Vadia S, Tse JL, Lucena R, Yang Z, Kellogg DR, Wang JD, Levin PA. 2017. Fatty acid availability sets cell envelope capacity and dictates microbial cell size. Curr Biol 27:1757–1767.e5. https://doi.org/10.1016/j.cub.2017.05.076.
28. Cronan JE. 2006. A family of arabinose-inducible Escherichia coli expression vectors having pBR322 copy control. Plasmid 55:152–157. https://doi.org/10.1016/j.plasmid.2005.07.001.
29. Welch RA, Burland V, Plunkett G, Redford P, Roesch P, Rasko D, Buckles EL, Liou SR, Boutin A, Hackett J, Stroud D, Mayhew GF, Rose DJ, Zhou S, Schwartz DC, Perna NT, Mobley HLT, Donnenberg MS, Blattner FR. 2002. Extensive mosaic structure revealed by the complete genome sequence of uropathogenic Escherichia coli. Proc Natl Acad Sci U S A 99:17020–17024. https://doi.org/10.1073/pnas.252529799.
30. Forde BM, Ben Zakour NL, Stanton-Cook M, Phan MD, Totsika M, Peters KM, Chan KG, Schembri MA, Upton M, Beatson SA. 2014. The complete genome sequence of Escherichia coli EC958: a high quality reference sequence for the globally disseminated multidrug resistant E. coli O25b:H4-ST131 clone. PLoS One 9:e104400. https://doi.org/10.1371/journal.pone.0104400.
31. Giske CG, Turnidge J, Cantón R, Kahlmeter G. 2022. Update from the European Committee on Antimicrobial Susceptibility Testing (EUCAST). J Clin Microbiol 60:e00276-21. https://doi.org/10.1128/JCM.00276-21.
32. Horne JE, Brockwell DJ, Radford SE. 2020. Role of the lipid bilayer in outer membrane protein folding in Gram-negative bacteria. J Biol Chem 295:10340–10367. https://doi.org/10.1074/jbc.REV120.011473.
33. Martinez E, Bartolomé B, de la Cruz F. 1988. pACYC184-derived cloning vectors containing the multiple cloning site and lacZα reporter gene of pUC8/9 and pUC18/19 plasmids. Gene 68:159–162. https://doi.org/10.1016/0378-1119(88)90608-7.
34. Mehta SC, Rice K, Palzkill T. 2015. Natural variants of the KPC-2 carbapenemase have evolved increased catalytic efficiency for ceftazidime hydrolysis at the cost of enzyme stability. PLoS Pathog 11:e1004949. https://doi.org/10.1371/journal.ppat.1004949.
35. O'Callaghan CH, Morris A, Kirby SM, Shingler AH. 1972. Novel method for detection of beta-lactamases by using a chromogenic cephalosporin

substrate. Antimicrob Agents Chemother 1:283–288. https://doi.org/10.1128/AAC.1.4.283.
36. Trautner BW, Darouiche RO. 2004. Role of biofilm in catheter-associated urinary tract infection. Am J Infect Control 32:177–183. https://doi.org/10.1016/j.ajic.2003.08.005.
37. Soto SM. 2014. Importance of biofilms in urinary tract infections: new therapeutic approaches. Advances in Biology 2014:1–13. https://doi.org/10.1155/2014/543974.
38. WHO. 2015. WHO estimates of the global burden of foodborne diseases: foodborne disease burden epidemiology reference group 2007–2015. WHO, Geneva, Switzerland.
39. Williams D. 2016. Antimicrobial resistance: are we at the dawn of the post-antibiotic era. J R Coll Physicians Edinb 46:150–156. https://doi.org/10.4997/JRCPE.2016.302.
40. Mahase E. 2019. Use some antibiotics more and others less to stem resistance, says WHO. BMJ 365:4282. https://doi.org/10.1136/bmj.l4282.
41. Ferenci T, Phan K. 2015. How porin heterogeneity and trade-offs affect the antibiotic susceptibility of Gram-negative bacteria. Genes 6:1113–1124. https://doi.org/10.3390/genes6041113.
42. Vaara M. 2019. Polymyxin derivatives that sensitize Gram-negative bacteria to other antibiotics. Molecules 24:249. https://doi.org/10.3390/molecules24020249.
43. Klobucar K, French S, Côté JP, Howes JR, Brown ED. 2020. Genetic and chemical-genetic interactions map biogenesis and permeability determinants of the outer membrane of Escherichia coli. mBio 11:e00161-20. https://doi.org/10.1128/mBio.00161-20.
44. MacNair CR, Brown ED. 2020. Outer membrane disruption overcomes intrinsic, acquired, and spontaneous antibiotic resistance. mBio 11: e01615-20. https://doi.org/10.1128/mBio.01615-20.
45. Stokes JM, MacNair CR, Ilyas B, French S, Côté JP, Bouwman C, Farha MA, Sieron AO, Whitfield C, Coombes BK, Brown ED. 2017. Pentamidine sensitizes Gram-negative pathogens to antibiotics and overcomes acquired colistin resistance. Nat Microbiol 2:17028. https://doi.org/10.1038/nmicrobiol.2017.28.
46. Yao J, Rock CO. 2017. Bacterial fatty acid metabolism in modern antibiotic discovery. Biochim Biophys Acta Mol Cell Biol Lipids 1862:1300–1309. https://doi.org/10.1016/j.bbalip.2016.09.014.
47. Logan LK, Weinstein RA. 2017. The epidemiology of carbapenem-resistant Enterobacteriaceae: the impact and evolution of a global menace. J Infect Dis 215:S28–S36. https://doi.org/10.1093/infdis/jiw282.
48. Lai C-Y, Cronan JE. 2003. β-Ketoacyl-acyl carrier protein synthase III (FabH) is essential for bacterial fatty acid synthesis. J Biol Chem 278: 51494–51503. https://doi.org/10.1074/jbc.M308638200.
49. Sanyal R, Singh V, Harinarayanan R. 2019. A novel gene contributing to the initiation of fatty acid biosynthesis in Escherichia coli. J Bacteriol 201: e00354-19. https://doi.org/10.1128/JB.00354-19.
50. Whaley SG, Radka CD, Subramanian C, Frank MW, Rock CO. 2021. Malonyl-acyl carrier protein decarboxylase activity promotes fatty acid and cell envelope biosynthesis in Proteobacteria. J Biological Chemistry 297: 101434. https://doi.org/10.1016/j.jbc.2021.101434.
51. Westfall C, Flores-Mireles AL, Robinson JI, Lynch AJL, Hultgren S, Henderson JP, Levin PA. 2019. The widely used antimicrobial triclosan induces high levels of antibiotic tolerance in vitro and reduces antibiotic efficacy up to 100-fold in vivo. Antimicrob Agents Chemother 63:e02312-18. https://doi.org/10.1128/AAC.02312-18.
52. Sinha AK, Winther KS, Roghanian M, Gerdes K. 2019. Fatty acid starvation activates RelA by depleting lysine precursor pyruvate. Mol Microbiol 112: 1339–1349. https://doi.org/10.1111/mmi.14366.
53. Rodionov DG, Ishiguro EE. 1995. Direct correlation between overproduction of guanosine 3',5'-bispyrophosphate (ppGpp) and penicillin tolerance in Escherichia coli. J Bacteriol 177:4224–4229. https://doi.org/10.1128/jb.177.15.4224-4229.1995.
54. Dalebroux ZD, Svensson SL, Gaynor EC, Swanson MS. 2010. ppGpp conjures bacterial virulence. Microbiol Mol Biol Rev 74:171–199. https://doi.org/10.1128/MMBR.00046-09.
55. Rodionov DG, Ishiguro EE. 1996. Dependence of peptidoglycan metabolism on phospholipid synthesis during growth of Escherichia coli. Microbiology 142:2871–2877. https://doi.org/10.1099/13500872-142-10-2871.
56. Kusser W, Ishiguro EE. 1985. Involvement of the relA gene in the autolysis of Escherichia coli induced by inhibitors of peptidoglycan biosynthesis. J Bacteriol 164:861–865. https://doi.org/10.1128/jb.164.2.861-865.1985.
57. Honsa ES, Cooper VS, Mhaissen MN, Frank M, Shaker J, Iverson A, Rubnitz J, Hayden RT, Lee RE, Rock CO, Tuomanen EI, Wolf J, Rosch JW. 2017. RelA mutant Enterococcus faecium with multiantibiotic tolerance arising in an immunocompromised host. mBio 8:e02124-16. https://doi.org/10.1128/mBio.02124-16.
58. Janßen HJ, Steinbüchel A. 2014. Fatty acid synthesis in Escherichia coli and its applications towards the production of fatty acid based biofuels. Biotechnol Biofuels 7:7. https://doi.org/10.1186/1754-6834-7-7.
59. Magnuson K, Jackowski S, Rock CO, Cronan JE Jr, 1993. Regulation of fatty acid biosynthesis in Escherichia coli. Microbiol Rev 57:522–542. https://doi.org/10.1128/mr.57.3.522-542.1993.
60. Simpson BW, Douglass MV, Trent MS. 2020. Restoring balance to the outer membrane: YejM's role in LPS regulation. mBio 11:e02624-20. https://doi.org/10.1128/mBio.02624-20.
61. Partridge SR, Ginn AN, Wiklendt AM, Ellem J, Wong JSJ, Ingram P, Guy S, Garner S, Iredell JR. 2015. Emergence of blaKPC carbapenemase genes in Australia. Int J Antimicrob Agents 45:130–136. https://doi.org/10.1016/j.ijantimicag.2014.10.006.
62. Datsenko KA, Wanner BL. 2000. One-step inactivation of chromosomal genes in Escherichia coli K-12 using PCR products. Proc Natl Acad Sci U S A 97:6640–6645. https://doi.org/10.1073/pnas.120163297.
63. Sarkar S, Hutton ML, Vagenas D, Ruter R, Schuller S, Lyras D, Schembri MA, Totsika M. 2018. Intestinal colonization traits of pandemic multidrug-resistant Escherichia coli ST131. J Infect Dis 218:979–990. https://doi.org/10.1093/infdis/jiy031.
64. Hong Y, Reeves PR. 2014. Diversity of O-antigen repeat unit structures can account for the substantial sequence variation of Wzx translocases. J Bacteriol 196:1713–1722. https://doi.org/10.1128/JB.01323-13.
65. Nikaido H. 2005. Restoring permeability barrier function to outer membrane. Chem Biol 12:507–509. https://doi.org/10.1016/j.chembiol.2005.05.001.
66. Muheim C, Götzke H, Eriksson AU, Lindberg S, Lauritsen I, Nørholm MH, Daley DO. 2017. Increasing the permeability of Escherichia coli using MAC13243. Sci Rep 7:1–11. https://doi.org/10.1038/s41598-017-17772-6.
67. Malinverni JC, Silhavy TJ. 2009. An ABC transport system that maintains lipid asymmetry in the Gram-negative outer membrane. Proc Natl Acad Sci U S A 106:8009–8014. https://doi.org/10.1073/pnas.0903229106.
68. Papp-Wallace KM, Taracila M, Hornick JM, Hujer AM, Hujer KM, Distler AM, Endimiani A, Bonomo RA. 2010. Substrate selectivity and a novel role in inhibitor discrimination by residue 237 in the KPC-2 beta-lactamase. Antimicrob Agents Chemother 54:2867–2877. https://doi.org/10.1128/AAC.00197-10.
69. Mobley HL, Green DM, Trifillis AL, Johnson DE, Chippendale GR, Lockatell CV, Jones BD, Warren JW. 1990. Pyelonephritogenic Escherichia coli and killing of cultured human renal proximal tubular epithelial cells: role of hemolysin in some strains. Infect Immun 58:1281–1289. https://doi.org/10.1128/iai.58.5.1281-1289.1990.
70. Sarkar S, Roberts LW, Phan MD, Tan L, Lo AW, Peters KM, Paterson DL, Upton M, Ulett GC, Beatson SA, Totsika M, Schembri MA. 2016. Comprehensive analysis of type 1 fimbriae regulation in fimB-null strains from the multidrug resistant Escherichia coli ST131 clone. Mol Microbiol 101: 1069–1087. https://doi.org/10.1111/mmi.13442.